

Spin-glass Behavior with Short-range Antiferromagnetic Order in Nd₂AgIn₃

著者	Li D. X., Nimori S., Shiokawa Y., Tobo A., Onodera H., Haga Y., Yamamoto E., Onuki Y.
journal or publication title	Applied Physics Letters
volume	79
number	25
page range	4183-4185
year	2001
URL	http://hdl.handle.net/10097/47003

doi: 10.1063/1.1428114

Spin-glass behavior with short-range antiferromagnetic order in Nd_2AgIn_3

D. X. Li,^{a)} S. Nimori,^{b)} and Y. Shiokawa

Institute for Materials Research, Tohoku University, Oarai, Ibaraki 311-1313, Japan

A. Tobo and H. Onodera

Institute for Materials Research, Tohoku University, Sendai 980-8577, Japan

Y. Haga, E. Yamamoto, and Y. Ōnuki

Advanced Science Research Center, Japan Atomic Energy Research Institute, Tokai, Ibaraki 319-1195, Japan

(Received 13 August 2001; accepted for publication 13 October 2001)

We present experimental results of complex susceptibility, static magnetization, magnetic relaxation, specific heat, and electrical resistivity measurements on an intermetallic compound Nd_2AgIn_3 . The results indicated that Nd_2AgIn_3 undergoes a spin-glass transition at a freezing temperature $T_f = 12.6$ K accompanied with the formation of short-range antiferromagnetic order. The mechanism of formation of spin-glass state in Nd_2AgIn_3 is different from that in diluted metallic spin-glass or uranium intermetallic compound. The existences of frustrated moments due to the triangles of nearest neighbors in Nd atomic layers and randomly distributed Ruderman–Kittle–Kasuya–Yosida interactions may be responsible for the spin glass state formed in Nd_2AgIn_3 . © 2001 American Institute of Physics. [DOI: 10.1063/1.1428114]

It has been commonly believed that competing between ferromagnetic (F) and antiferromagnetic (AF) near-neighbor interactions caused by randomly varying bond angles and interatomic distances is mainly responsible for the formation of spin-glass (SG) state in amorphous or diluted metallic SG materials. Nonmagnetic atom disorder (NMAD) spin glasses such as URh_2Ge_2 (Ref. 1) and PrAu_2Si_2 (Ref. 2) reported earlier, however, are crystallographically ordered substances. In such systems, the origin of SG behavior depending on the disorder at the nonmagnetic sites is evidently different from that in amorphous or diluted metallic spin glass. We have observed the SG behavior for ternary intermetallic compounds of uranium U_2TSi_3 (T=transition metal), and suggested that the $5f$ -ligand hybridization may be mainly responsible for the observed SG behavior.^{3–6} In addition, for rare earth compound, since the $4f$ state is well localized, the $4f$ -ligand hybridization is usually considered to be much weaker. Thus to clarify the mechanism of SG behavior in rare earth NMAD spin glass has been a subject of intensive studies during the past several years.⁷ Recently, we have been paying special attention to a new family of the 2:1:3 compounds, namely R_2AgIn_3 (R=rare-earth element). Up to now, the systematic measurements of thermal, magnetic, and transport properties of R_2AgIn_3 compounds are reported only for Ce_2AgIn_3 that shows the canonical SG behavior below a very low spin freezing temperature $T_f = 1.8$ K.⁸ In this letter, we present basic physical properties of polycrystalline Nd_2AgIn_3 . Our experimental results suggest that Nd_2AgIn_3 is not a “simple” spin glass. The occurrence of SG behavior in this system is accompanied by the formation of short-range AF order.

The polycrystalline sample of Nd_2AgIn_3 was prepared

by arc melting of stoichiometric amounts of the constituent elements in argon atmosphere. To ensure homogeneity the ingot was remelted several times and annealed at 750 °C for two weeks in an evacuated quartz tube and then water-quenched. The x-ray-diffraction pattern of this sample can be completely indexed based on the disordered hexagonal CaIn_2 -type structure model (space group $P6_3/mmc$) with room-temperature lattice constants $a = 4.8826$ Å and $c = 7.5841$ Å. The complex susceptibility (ac susceptibility), static magnetization (dc magnetization), and magnetic relaxation were measured using a Quantum Design superconducting quantum interference device (SQUID) magnetometer. After a *reset magnet operation* is performed, the remnant field of the magnet in the SQUID is about 0.7 Oe as determined by using a standard palladium sample. The adiabatic heat pulse method was employed for specific heat measurements over the temperature range between 1.7 and 42 K. Electrical resistivity measurement was performed between 4.2 and 284 K using a standard four-terminal method.

Figure 1 shows the temperature dependence of the real component (χ'_{ac}) of the ac susceptibility of Nd_2AgIn_3 between 10 and 20 K at the frequency range $0.1 \leq \nu \leq 1000$ Hz. χ'_{ac} exhibits a pronounced maximum with amplitude and position [$T_f(\nu)$] depending on the frequency of the applied magnetic field. The initial frequency shift $\delta T_f = \Delta T_f / (T_f \Delta \log \nu)$ is determined to be 0.015 ± 0.001 . This value is comparable to those reported for other metallic SG systems, e.g., AuFe: 0.010,⁹ U_2RhSi_3 : 0.008,⁶ URh_2Ge_2 : 0.025,¹ and Ce_2AgIn_3 : 0.022.⁸ As shown by a solid line in the inset of Fig. 1, our experimental data for Nd_2AgIn_3 could be fitted well using the empirical Vogel–Fulcher law, $\nu = \nu_0 \exp[-E_a/k_B(T_f - T_0)]$, with three fitting parameters: characteristic frequency ν_0 , activation energy E_a (k_B is the Boltzmann constant), and Vogel–Fulcher temperature T_0 . Following Tholence,¹⁰ $\nu_0 = 10^{13}$ Hz was kept fixed, the best fit to this equation yields the fitting parameters E_a/k_B and T_0

^{a)}Electronic mail: dxli@imr.tohoku.ac.jp

^{b)}Also at: Tsukuba Magnet Laboratory, National Research Institute for Metals, 3-13 Sakura, Tsukuba 305-0003, Japan.

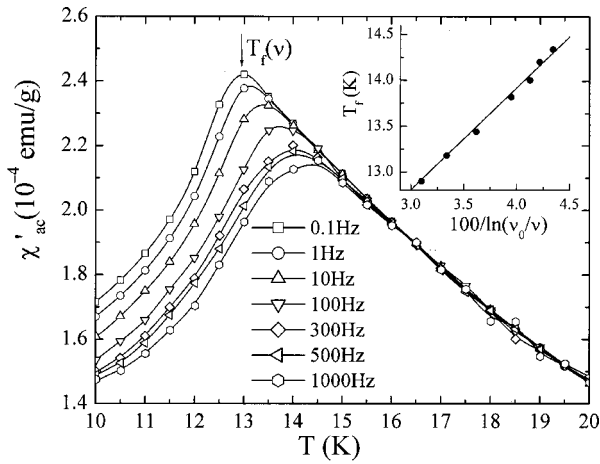


FIG. 1. Real component χ'_{ac} of the ac susceptibility of Nd_2AgIn_3 vs temperature between 10 and 20 K at frequencies $0.1 \leq \nu \leq 1000$ Hz in an applied ac field of 5 Oe. The inset shows the plot of T_f vs $(100 \ln \nu_0/\nu)$ with $\nu_0 = 10^{13}$ Hz.

to be 11.4 and 9.7 K, respectively. These results indicate the formation of SG state in Nd_2AgIn_3 .

The temperature dependence of the dc magnetization $M(T)$ of Nd_2AgIn_3 is measured in magnetic fields between 0.01 and 10 kOe under the zero-field cooling (ZFC) mode and the field-cooling (FC) mode, respectively. A part of the results is shown in Fig. 2. There exists a characteristic temperature $T_f(H)$, below which a difference is observed between the M_{ZFC}/H and the M_{FC}/H curves, indicating the appearance of irreversibility. This irreversible magnetism is a typical feature of SG system. In a field of 10 Oe, the M_{ZFC}/H curve exhibits a sharp peak at the temperature very near to $T_f = 12.6$ K. With increasing H , this peak becomes broader and its height decreases, while $T_f(H)$ shifts toward lower temperatures. The inset of Fig. 2 shows the de Almeida–Thouless (AT) line for Nd_2AgIn_3 . $T_f(H)$ follows an $H^{2/3}$ law, which has also been observed in SG systems of UCuSi^{11} and U_2PdSi_3 ,³ and has also been predicted by the mean-field SG model.¹² For a spin glass, the spin freezing temperature T_f is a function of ν and H , and generally defined as either the peak temperature of χ'_{ac} in ac susceptibility

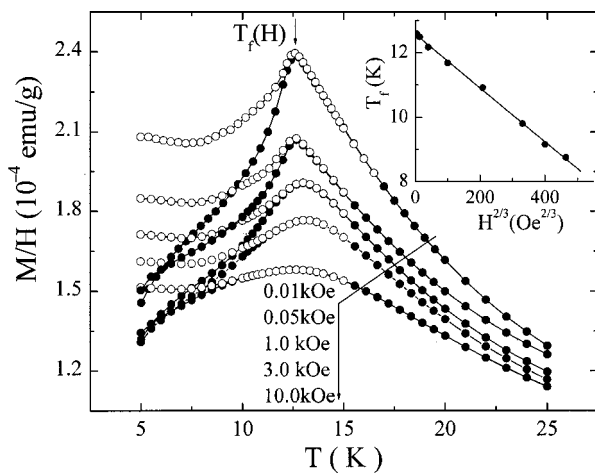


FIG. 2. Magnetization data M/H vs temperature for Nd_2AgIn_3 measured in the FC (○) mode and in the ZFC (●) mode in various magnetic fields. The inset shows the field dependence of the spin-glass transition temperature T_f , plotted as T_f vs $H^{2/3}$.

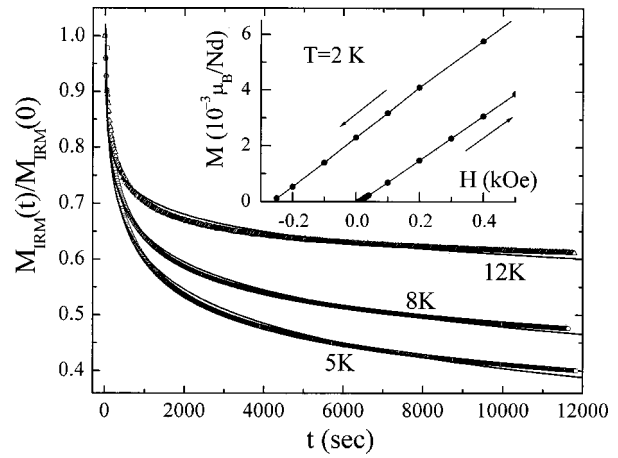


FIG. 3. Isothermal remanent magnetization $M_{\text{IRM}}(t)$ as a function of time t at 5, 8, and 12 K for Nd_2AgIn_3 plotted as $M_{\text{IRM}}(t)/M_{\text{IRM}}(0)$ vs t . The solid lines represent “least-squares” fits using the expression $M_{\text{IRM}}(t) = M_0(T) - \alpha(T) \ln(t)$. The inset displays the $M(H)$ data around 0 Oe in an expanded scale measured at 2 K after ZFC the sample from 100 K.

measurement or the temperature where the irreversibility appears in dc magnetization measurement. In the case of Nd_2AgIn_3 , T_f is determined to be 12.6 K in $H = 10$ Oe from Fig. 2.

The magnetic field dependence of magnetization was measured at 2 K in magnetic field up to 10 kOe for the Nd_2AgIn_3 sample that was cooled down from 100 K under the ZFC mode. The remanence effect is clearly shown in the inset of Fig. 3 around 0 Oe in an expanded scale. The magnetic relaxation of Nd_2AgIn_3 was studied by measuring the isothermal remanent magnetization M_{IRM} as a function of time t at temperatures below T_f . First, we cooled the sample in zero field from 100 K (far above T_f) to the desired temperature, then a magnetic field of 5 kOe was applied for 5 min and switched off in 2 min. M_{IRM} of Nd_2AgIn_3 decays so slowly that a nonzero value could still be detected after 3 h (see Fig. 3). Solid lines in Fig. 3 correspond to a fit to the observed time dependence of M_{IRM} of Nd_2AgIn_3 using the expression $M_{\text{IRM}}(t) = M_0(T) - \alpha(T) \ln(t)$. The results for the two temperature dependent fitting parameters are $M_0(T) = 4.481 \times 10^{-2}$, 3.996×10^{-2} , and 5.235×10^{-3} emu/g, and $\alpha(T) = 3.244 \times 10^{-3}$, 2.522×10^{-3} and 2.285×10^{-4} emu/g for $T = 5, 8,$ and 12 K, respectively.

Other important evidence of the SG state formed in Nd_2AgIn_3 is specific heat (C_1 , closed circles in Fig. 4) and electrical resistivity (ρ , not shown here) measurements. The absence of any dramatic change in $C_1(T)$ and $\rho(T)$ around $T_f = 12.6$ K excludes the existence of long-range spatial magnetic ordering at T_f , which is in consistent with the recent neutron diffraction results.¹³ It is interesting to note that compared with the canonical SG behavior observed for Ce_2AgIn_3 (Ref. 8) and U_2PdSi_3 ,³ the magnetic properties of Nd_2AgIn_3 around the spin freezing temperature T_f cannot be explained by a simple SG model, because an evident decrease in $M_{\text{FC}}(T)$ can be observed below T_f , as shown in Fig. 2. In contrast, $M_{\text{FC}}(T)$ for a canonical spin glass tends to be nearly constant below T_f . It seems that a short-range antiferromagnetic order (i.e., AF cluster) occurs at the temperature near T_f , which is confirmed by the magnetization (M , Fig. 4 inset) and specific heat (C_2 , open circles in Fig. 4) measurements. The magnetic field dependence of magnetization was measured at 2 K in magnetic field up to 10 kOe for the Nd_2AgIn_3 sample that was cooled down from 100 K under the ZFC mode. The remanence effect is clearly shown in the inset of Fig. 3 around 0 Oe in an expanded scale. The magnetic relaxation of Nd_2AgIn_3 was studied by measuring the isothermal remanent magnetization M_{IRM} as a function of time t at temperatures below T_f . First, we cooled the sample in zero field from 100 K (far above T_f) to the desired temperature, then a magnetic field of 5 kOe was applied for 5 min and switched off in 2 min. M_{IRM} of Nd_2AgIn_3 decays so slowly that a nonzero value could still be detected after 3 h (see Fig. 3). Solid lines in Fig. 3 correspond to a fit to the observed time dependence of M_{IRM} of Nd_2AgIn_3 using the expression $M_{\text{IRM}}(t) = M_0(T) - \alpha(T) \ln(t)$. The results for the two temperature dependent fitting parameters are $M_0(T) = 4.481 \times 10^{-2}$, 3.996×10^{-2} , and 5.235×10^{-3} emu/g, and $\alpha(T) = 3.244 \times 10^{-3}$, 2.522×10^{-3} and 2.285×10^{-4} emu/g for $T = 5, 8,$ and 12 K, respectively.

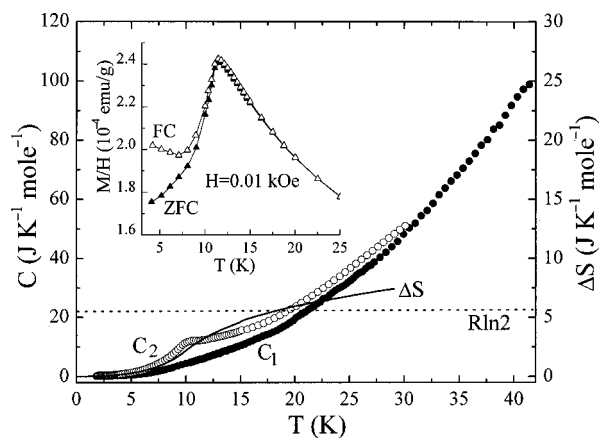


FIG. 4. Temperature dependencies of specific heats of Nd_2AgIn_3 samples annealed at 750°C for two weeks (C_1 : \bullet) and annealed at 850°C for two weeks (C_2 : \circ) between 1.7 and 42 K. The solid line shows the calculated additional entropy ΔS for the high-temperature annealed sample using the data $\Delta C = C_2 - C_1$. The inset illustrates the FC and ZFC magnetization data M/H vs T in a magnetic field of 0.01 kOe for the high-temperature annealed sample.

Fig. 4) measurements performed for a high-temperature-annealed (at 850°C for two weeks) Nd_2AgIn_3 sample. The peak in $M_{\text{FC}}(T)$ is evidently larger in comparison to that shown in Fig. 3; $C_2(T)$ shows a rise at about 11 K followed by a small and broad peak around 10.5 K. The solid line in Fig. 4 shows the calculated additional entropy $\Delta S(T)$ for the high-temperature-annealed sample using the data $\Delta C(T) = C_2(T) - C_1(T)$. Even if ΔS is considered to result completely from the additional magnetic contribution, the specific heat anomaly near 10.5 K contains a smaller amount of magnetic entropy per Nd atom $\Delta S/(2R) = 0.19 = 0.27 \ln 2$ (R is the gas constant), indicating that long-range AF order is not formed even in the high-temperature-annealed sample. The magnetic cluster effect may be responsible for the specific heat anomaly. These results suggest that magnetic clusters in Nd_2AgIn_3 could extend in size after annealing the sample at a suitably high temperature for a long time.

One necessary condition for formation of a SG state is the existence of frustration.¹⁴ Nd_2AgIn_3 has a CaIn_2 -type structure, which consists of layers of magnetic Nd atoms alternating with nonmagnetic Ag–In layers along the c axis. Within one magnetic layer, Nd atoms form triangles of nearest neighbors. Hence frustration of the magnetic interactions could be induced by this topology in the case of AF coupling between nearest neighbors. The neutron diffraction study for Tb_2AgIn_3 has shown the existence of competition between F and AF interactions within Tb layers.¹⁵ Similar competing magnetic interactions and thus frustrated magnetic moments of Nd atoms could be expected in Nd_2AgIn_3 due to the isostructuralism. Another necessary condition to achieve a SG state is randomness.¹⁴ It means that the distribution of F and AF interactions between magnetic atoms must be at least partially random. In Nd_2AgIn_3 , randomness could arise only from the statistical distribution of the Ag and In positions similar to the cases of U_2TSi_3 .^{3–6} As described previously,

however, the mechanism of SG behavior observed in NMAD rare earth compound is evidently different from that observed in diluted metallic spin glass or in NMAD uranium compound due to the crystallographic order and much weaker $4f$ -ligand hybridization. We believe that periodic space structure of the conduction band does not exist in Nd_2AgIn_3 , since the randomly situated Ag and In atoms vary the electronic environment around the Nd atoms. Such disorder band structure could cause a distribution of Ruderman–Kittle–Kasuya–Yosida (RKKY) interactions, that is, random bond between Nd ions in this system.

In conclusion, our results of ac susceptibility, dc magnetization, magnetic relaxation, specific heat, and electrical resistivity measurements on a polycrystalline Nd_2AgIn_3 showed typical SG features at low temperature with short-range AF order. This is consistent with the neutron diffraction results that suggest the nonexistence of long-range magnetic order in this compound.¹³ The origin of SG behavior for Nd_2AgIn_3 is different from that in diluted metallic spin glass or uranium intermetallic compound. The frustrated magnetic moments may be originated in Nd_2AgIn_3 from the competing between F and AF interactions in Nd-atom layer in which nearest-neighbor Nd atoms form triangular structure. On the other hand, the statistical distribution of Ag and In atoms could introduce the randomly distributed RKKY-type magnetic exchange interactions. Both the frustration and randomness are necessary for the occurrence of the SG state.

- ¹S. Süllow, G. J. Nieuwenhuys, A. A. Menovsky, J. A. Mydosh, S. A. M. Mentink, T. E. Mason, and W. J. L. Buyers, *Phys. Rev. Lett.* **78**, 354 (1997).
- ²A. Krimmel, J. Hemberger, M. Nicklas, C. Knebel, W. Trinkl, M. Brando, V. Fritsch, and A. Loidl, *Phys. Rev. B* **59**, R6604 (1999).
- ³D. X. Li, Y. Shiokawa, Y. Homma, A. Uesawa, A. Dönni, T. Suzuki, Y. Haga, E. Yamamoto, T. Homma, and Y. Onuki, *Phys. Rev. B* **57**, 7434 (1998).
- ⁴D. X. Li, Y. Shiokawa, Y. Homma, A. Uesawa, and T. Suzuki, *J. Magn. Magn. Mater.* **176**, 261 (1997).
- ⁵D. X. Li, A. Kimura, Y. Homma, Y. Shiokawa, A. Uesawa, and T. Suzuki, *Solid State Commun.* **108**, 863 (1998).
- ⁶D. X. Li, A. Dönni, Y. Kimura, Y. Shiokawa, Y. Homma, Y. Haga, E. Yamamoto, T. Homma, and Y. Onuki, *J. Phys.: Condens. Matter* **11**, 8263 (1999).
- ⁷For examples, see J. S. Hwang, K. J. Lin, and C. Tien, *Solid State Commun.* **100**, 169 (1996); C. Tien, C. H. Feng, C. Shui, and J. J. Lu, *Phys. Rev. B* **61**, 12151 (2000); A. Szytuła, M. Hofmann, B. Penc, M. Slaski, S. Majumdar, E. V. Sampathkumaran, and A. Zygmunt, *J. Magn. Magn. Mater.* **202**, 365 (1999); I. M. Siouris, I. P. Semitelou, J. K. Yakinthos, W. Schäfer, and R. R. Arons, *J. Alloys Compd.* **314**, 1 (2001).
- ⁸T. Nishioka, Y. Tabata, T. Taniguchi, and Y. Miyako, *J. Phys. Soc. Jpn.* **69**, 1012 (2000).
- ⁹J. A. Mydosh, *Spin Glass: An Experimental Introduction* (Taylor & Francis, London, 1993).
- ¹⁰J. L. Tholence, *Solid State Commun.* **35**, 113 (1980).
- ¹¹V. H. Tran and R. Troc, *J. Magn. Magn. Mater.* **86**, 231 (1990).
- ¹²J. R. L. de Almeida and D. J. Thouless, *J. Phys. A* **11**, 983 (1978).
- ¹³J. Siouris, J. P. Semitelou, J. K. Yakinthos, and W. Schäfer, *Physica B* **276–278**, 582 (2000).
- ¹⁴K. Binder and A. P. Young, *Rev. Mod. Phys.* **58**, 801 (1986).
- ¹⁵J. P. Semitelou, J. Siouris, J. K. Yakinthos, W. Schäfer, and D. Schmitt, *J. Alloys Compd.* **283**, 12 (1999).